

# Measurement of Branching Ratio for broad 27-keV Resonance of $^{19}\text{F}(\text{n},\text{g})^{20}\text{F}$ Reaction by using Time-of-flight Method with Anti-Compton NaI(Tl) Spectrometer

Samyol Lee

*Nambu University, Department of Radiological Science*

## Abstract

The neutron capture spectrum for the light nuclide was very useful to study the nuclear structure. In the present study, the capture gamma-ray from the 27-keV resonance of  $^{19}\text{F}(\text{n},\text{g})^{20}\text{F}$  reaction were measured with an anti-Compton NaI(Tl) spectrometer and the 3-MV Pelletron accelerator of the Research Laboratory for Nuclear Reactors at the Tokyo institute of technology. A neutron Time-of-Flight method was adopted with a 1.5 ns pulsed neutron source by the  $^7\text{Li}(\text{p},\text{n})^7\text{Be}$  reaction. In the present experiment, a Teflon( $(\text{CF}_2)_n$ ) sample was used. The sample was disk with a diameter of 90mm. The thickness of sample was determined so that reasonable counting rates could be obtained and the correction was not so large for the self-shielding and multiple scattering of neutrons in the sample, and was 5mm. The primary gamma-ray transitions were compared with previous measurement of Kenny.

## I. Introduction

Neutron capture gamma-ray spectroscopy is the single most powerful tool for experimental study of the odd-odd nuclei. Until now, Many experiments have been extensively carried out  $^{19}\text{F}(\text{n},\text{g})^{20}\text{F}$  reaction for thermal neutron. However, the data is not so many for keV-neutron capture reaction[1,2,3].

For the last decade, we have been measured capture gamma-rays from broad keV-neutron capture reaction in the  $A=20-40$  region to study resonance capture mechanisms[1,4] by using NaI(Tl) spectrometer. We started measurements of keV-neutron capture gamma-rays for odd-Z nuclei in the 2s-1d shell region by using an anti-Compton NaI(Tl) spectrometer that has large size, high detection efficiency.

The case of  $^{19}\text{F}$  sample is very interesting for this nucleus lies just above the group of nuclides ending

with  $^{16}\text{O}$  that has become filled in the 1p shell. We have measured keV-neutron capture gamma-rays from  $^{19}\text{F}(\text{n},\text{g})^{20}\text{F}$  reaction. While, this reaction in the keV-neutron energy region was studied by M. J. Kenny et al in 1974 year[5]. Their report was not enough of result to explain the reaction. Therefore, we select  $^{19}\text{F}(\text{n},\text{g})^{20}\text{F}$  reaction for supplying of their data. A Teflon( $\text{C}_2\text{F}_4$ ) target was used for measuring.

We can obtained several primary transition gamma-rays from 27-keV neutron resonance from the reaction. We can obtained relative intensity of each primary gamma-ray.

## II. Experiment

The measurement was performed in the two neutron energy region of 10 to 80 keV using the 3-MV Pelletron accelerator of the Research Laboratory for Nuclear Reactors at the Tokyo Institute of Technology.

The experimental arrangement is shown in Fig. 1. Pulsed keV neutrons were produced by the  ${}^7\text{Li}(p,n){}^7\text{Be}$  reaction, using a 1.5-ns bunched proton beam from the Pelletron accelerator. The incident neutron spectrum on a capture sample was measured by means of a time-of-flight (TOF) method with a  ${}^6\text{Li}$ -glass scintillation detector. The capture sample was located at an angle of  $0^\circ$  with respect to the proton beam direction. Capture gamma rays were detected with an anti-Compton NaI(Tl) spectrometer, employing a TOF method. Capture events detected by the spectrometer were stored in a workstation as two-dimensional data on TOF and pulse height (PH).

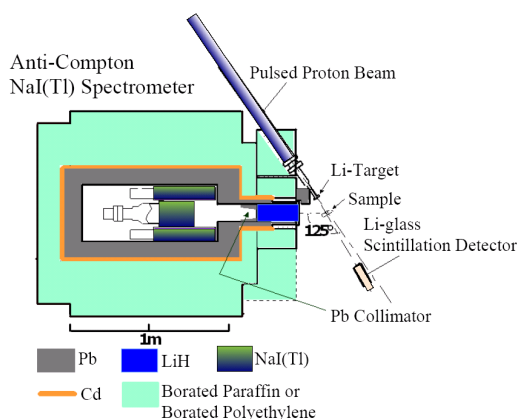


Figure 1. Experimental Arrangement.

A thick lithium target was made by evaporating metallic lithium on a copper disk with a diameter of 3.0cm and a thickness of 0.4mm. The diameter of lithium layer was about 2.0cm. After evaporating lithium on the disk, the lithium target was cooled down to the room temperature in a vacuum of about  $1\cdot 10^{-4}$  Pa. Then, the target was put into a balloon filled with dry nitrogen gas to prevent lithium from oxidizing and/or hydrating, and was carried to a neutron target holder at the end of beam line. Finally, the target was mounted on the holder filled with the gas, and a turbo-molecular pump evacuated the holder quickly. The oxidization and/or hydration of lithium make the layer thick in a measure of energy loss of incident

proton, and cause the decrease of neutron flux per unit neutron energy.

Pulsed keV neutrons were produced from the  ${}^7\text{Li}(p,n){}^7\text{Be}$  reaction by bombarding the thick lithium target with the 1.5-ns bunched proton beam from the Pelletron accelerator. A  ${}^6\text{Li}$ -glass scintillation detector was used as a neutron detector in the present experiment. Capture gamma rays were detected with a large anti-Compton NaI(Tl) spectrometer, employing a TOF method. The main NaI detector with a relative efficiency of 100% was centered in a 25.4cm outer diameter by 30.5cm NaI(Tl) annular Compton-suppression detector. The main NaI detector and annular NaI detector were shown in Fig. 1. A simplified block diagram of electronics for the gamma-ray spectrometer is shown in Fig. 2. The signal from the NaI detector was divided into three: the timing, PH, and PH-discrimination signals. The shaping time of Linear Amplifier(LA) longer than  $6\times 10^{-6}$ s was necessary for obtaining good energy resolution, while much shorter shaping time was necessary for reducing the time delay of TSCA. A pair of P.H. and T.O.F. signals were sent to individual A.D.C.s, and converted to a pair of digital P.H. and T.O.F. data, which were combined at a Mul.P.I/F.(Multi Parameter InterFace). The combined data were sent to a D.P.M.(Dual Port Memory). Another output signal from the U.C. was sent to a G.D.G. The signal from G.D.G. was fed into a Scaler for the measurement of the dead time. The output signals of D.P.M. and Scaler were sent to a Crate Controller through a CAMAC Bus, and finally, via a VME Bus, these signals were taken as two-dimensional data on TOF and PH, and stored into a workstation in a list mode. Here, the dead time was obtained by comparing the counts by the Scaler with the number of the events stored in the work station.

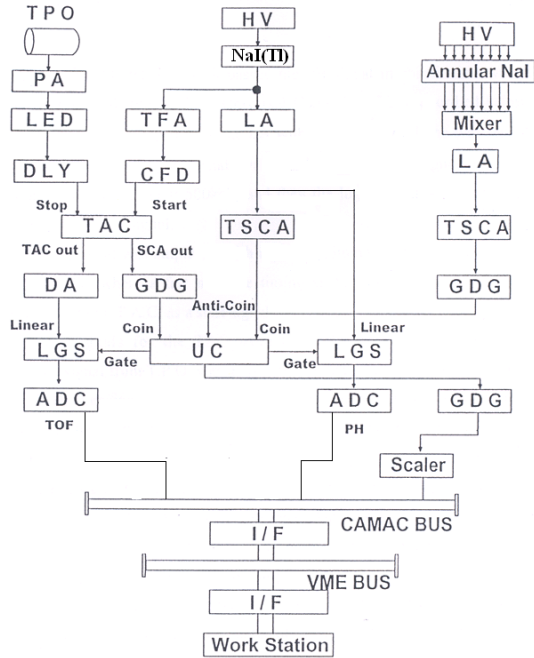


Figure 2. Block diagram for measurement of prompt gamma ray from the sample.

### III. Result and Conclusion

A part of two-dimensional spectrum of the PH and TOF signals from the gamma-ray spectrometer obtained for the F run in the 10-80 keV measurement is shown in Fig. 3. The TOF decreases with increasing channel number, because the reference pulses from the time pick-off unit were used as the stop signals of TAC. Its projected spectrum on the TOF axis (TOF spectrum) is shown in Fig. 3, where the bunching is not performed. The FWHM(Full Width Half Maximum) of the  $^7\text{Li}(p,g)^8\text{Be}$  peak was improved from 20ns to 12ns by the correction. The  $^{19}\text{F}(n,g)^{20}\text{F}$  events are well separated from the  $^7\text{Li}(p,ng)^8\text{Be}$  events but the separation among the neutron resonances is poor, as shown in Fig. 3.

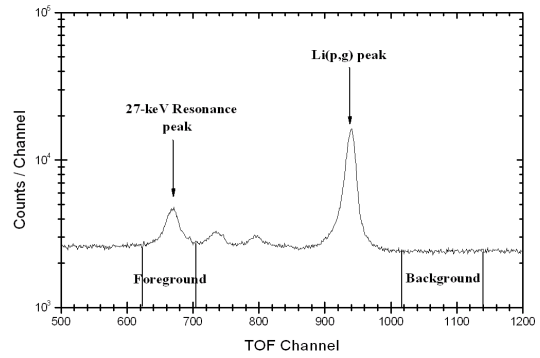


Figure 3. TOF spectrum observed with the gamma ray spectrometer for the F run in the 10-80 keV measurement.

The primary gamma ray from the 27-keV resonance were measured by gate to the resonance region of TOF spectrum. The result were shown in figure 4 and Table 1.

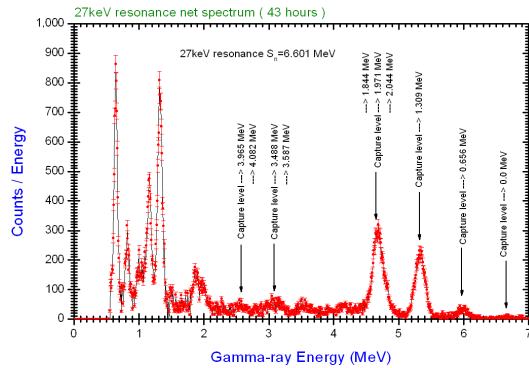


Figure 4. The primary gamma ray spectrum from the 27-keV resonance of  $^{19}\text{F}(n,g)^{20}\text{F}$  reaction.

In the present study, 10 primary gamma rays were measured by anti-compton NaI spectrometer. Although almost gamma rays were seem good agreement with previous Kenny's data [5], two primary gamma ray were different with the present result.

Table 1. The result of primary gamma ray from the 27-keV resonance of  $^{19}\text{F}(n,g)^{20}\text{F}$  reaction.

Final States (MeV)	$J\pi$	Relative Intensities(%)	
		Present	Kenny
0.000	$2^+$	$0.9 \pm 0.1$	$2.0 \pm 0.5$
0.656	$3^+$	$6.0 \pm 0.2$	$6 \pm 1$
0.984	$1^-$	—	—
1.057	$1^+$	—	—
1.309	$2^-$	$34 \pm 0.5$	$31 \pm 2$
1.844	$2^-$	$6.8 \pm 0.1$	$8 \pm 2$
1.971	$(3^-)$	$38 \pm 0.5$	$46 \pm 4$
2.044	$2^+$	$2.0 \pm 0.02$	$1.5 \pm 4$
2.194	$(3^+)$	$2.0 \pm 0.3$	—
3.489	$1^+$	$5.6 \pm 0.3$	$3 \pm 1$
3.526	$0^+$	—	—
3.587	$(1, 2^+)$	—	—
3.680	1, 2	—	—
3.965	$1^+$	$1.4 \pm 0.1$	—
4.082	$(1)^+$	$1.6 \pm 0.2$	$2.5 \pm 1$
4.315	$(0, 1)^+$	—	—
4.731	$(3^-, 4, 5^+)$	—	—
5.555	1, $2^+$	—	—

## Reference

- [1] Allen, B. J., Cohen, D. D., Company, F. Z.: J. Phys. G: Nucl. Phys., **6**, 1173 (1980).
- [2] Anttila, A., Keinonen, J., Hautala, M., Forsblom, I.: Nucl. Instrum. and Methods, **147**, 501 (1977).
- [3] Bergqvist, I., Biggerstaff, J. A., Gibbons, J. H., Good, W. M.: Phys. Rev., **158**, 1049 (1967).
- [4] Blatt J. M., Weisskopf V.F.: Theoretical Nuclear Physics, John Wiley & Sons, New York (1952).
- [5] Kenny, M. J., Martin, P. W., Carlson L. E., Biggerstaff, J. A.: Aust. J. Phys., **27**, 759 (1974).